Vietnam Journal of Biotechnology **21**(2): 197-217, 2023

IN SILICO SCREENING FOR ANTI-ZIKA VIRUS COMPOUNDS FROM *ECLIPTA PROSTRATA* BY MOLECULAR DOCKING

Thien-Hoang Ho[1,✉], Uyen-Thanh Nguyen Thi[1], Quoc-Dang Quan[2], Kim-Tuyen Nguyen Thi[2,3], Trang H. D. Nguyen[1], Dinh-Thach Bui[4]

[1]*Institute of Biotechnology and Food Technology, Industrial University of Ho Chi Minh City, 12 Nguyen Van Bao, Ward 4, Go Vap District, Ho Chi Minh City, Vietnam*
[2]*Thien Thanh Bio Co.,Ltd, 204/9 Truong Cong Dinh, Ward 14, Tan Binh District, Ho Chi Minh City, Vietnam*
[3]*Ho Chi Minh City University of Technology, 227 Ly Thuong Kiet, District 10, Vietnam*
[4]*Institute of Tropical Biology, 9/621 Hanoi Highway, Linh Trung Ward, Thu Duc City, Ho Chi Minh City, Vietnam*

✉To whom correspondence should be addressed. E-mail: hothienhoang@iuh.edu.vn

Received: 28.3.2023
Accepted: 24.4.2023

SUMMARY

Zika virus (ZIKV) belongs to the flavivirus family, and infection with ZIKV can lead to microcephaly, neurological issues like Guillain-Barré syndrome, and other birth defects. Zika virus can cause serious complications during pregnancy, such as delivery complications and pregnancy problems. It can also lead to severe illnesses, including swelling of the brain and spinal cord, as well as bleeding disorders. The Zika virus gained worldwide attention during the pandemic in Brazil, which led to extensive research efforts to discover effective and safe anti-Zika virus therapies. This study aimed to determine the efficacy of several bioactive compounds of plant origin against ZIKV NS5 RNA-dependent RNA polymerase (RdRp) (PDB ID: 5WZ3 and 5U04), ZIKV NS3 helicase (NS3h) (PDB ID: 5JRZ), Human tyrosine-protein kinase receptor UFO (Axl Receptor) (PDB ID: 2C5D), and human Axl Kinase (PDB ID: 5U6B). Fifty-three compounds from *Eclipta prostrata* (L.) were selected for screening based on the molecular docking method. The findings showed that these compounds inhibit ZIKV infection with high values of bond strength and free binding energy. AutoDock Vina results indicated that ecliptasaponin A exhibited the highest score value of -8.6 kcal/mol against the human Axl receptor, while eclalbasaponin I had the highest score value of -9.6 kcal/mol against ZIKV-NS2h. Additionally, echinocystic acid demonstrated the highest score value of -10.0 kcal/mol against ZIKV-NS5-RdRp (PDB: 5U04), while ursolic acid had the highest score of -9.9 kcal/mol against Axl kinase. Furthermore, it is noteworthy that ecliptasaponin, α-amyrin, ecliptasaponin A, and ursolic acid all had the highest score value of -9.9 kcal/mol against ZIKV-NS5-RdRp (PDB: 5WZ3). ADME prediction study found that echinocystic acid, eclalbasaponin I, and ecliptasaponin A have inhibitory abilities and are highly pharmacologically active, while α-amyrin and ursolic acid showed no results. However, all five substances are insoluble and lack optimal saturation, making oral absorption limited. These results in silico demonstrated

that the bioactive compound from *E. prostrata* exhibited strong potential for developing inhibitory drugs against Zika virus.

Keywords: Zika virus, molecular docking, NS3-helicase, NS5-RNA polymerase, Eclipta prostrata, ADME cytotoxicity

INTRODUCTION

Currently, there have been numerous outbreaks of diseases worldwide, caused by various viruses. The Zika virus (ZIKV) is one of these, having been first isolated in 1947 from an infected macaque found in the Zika forest of Uganda. The following year, the virus was found in Aedes mosquito in the same area. The first human cases of ZIKV were reported in 1952 in the United Republic of Tanzania and Uganda where neutralizing antibodies against the virus were detected in the serum of the patients (Dick *et al.*, 1952). In 1954, three patients in Eastern Nigeria were found to be infected with ZIKV during an outbreak of Jaundice (Macnamara, 1954; Marchette *et al.*, 1969). Around the same time, the virus was isolated from *Aedes africanus* in Africa and *Aedes aegypti* in Southeast Asian countries, especially in Malaysia (Haddow *et al.*, 1964). ZIKV serological studies conducted from 1954 to 1993 in different African countries, including Kenya, Sierra Leone, Gabon, the Central African Republic, and Senegal, confirmed its presence. In Asia, ZIKV was detected in acute febrile subjects from Central Java and Lombok Island in Indonesia. Since 2007 and up to the present time, there have been several occurrences of Zika virus outbreaks, characterized by manifestations such as rashes, headaches, red eyes, congenital abnormalities in infants born to infected mothers, and a link between viral infection and the emergence of neuroinflammatory syndromes such as Guillain-Barré syndrome (GBS), meningitis, and myelitis. So that, the constant threat of re-emerging viruses such as ZIKV in the 21st century highlights the urgent requirement for research and drug development to effectively combat this disease. (Maslow, Roberts, 2020).

Eclipta prostrata (L.) L., which is also known as *Eclipta alba* (L.) Hassak and belongs to the Asteraceae family, holds great significance as a medicinal plant in the tropical and subtropical regions. *E. prostrata* is a commonly used herb in traditional medicine, particularly in various parts of Asia, such as China, Korea, India, and Vietnam. It is known for its medicinal properties and is used for the treatment of various ailments. In traditional Chinese medicine, it is believed to have cooling and detoxifying effects on the liver, reduce inflammation, and promote the circulation of blood and Qi (life force energy). It is also used to treat digestive issues such as diarrhea and dysentery, as well as liver conditions such as jaundice and cirrhosis. In Vietnam, it is used as an anti-inflammatory agent for skin diseases and is also believed to have anti-cancer properties. The traditional use of *E. prostrata* in different parts of the world highlights its versatility and potential health benefits (Liu *et al.*, 2012). The research aimed to assess the effectiveness of various bioactive drug candidates derived from *E. prostrata* against ZIKV through the use of virtual screening techniques and various computational analyses.

MATERIALS AND METHODS

Chemical compounds from *E. prostrata*

Fifty-three compounds from *E. prostrata* were subjected to evaluate the interaction with Zika RNA-dependent RNA polymerase, ZIKA NS3 helicase (NS3h) enzyme, human Axl Receptor, and human Axl protein (Ogunbinu *et al.*, 2009).

Molecular docking analysis

Molecular docking was conducted using Autodock software. While there are some alternative tools, Autodock software was employed due to its established reputation and its accurate illustration of the ligand in the pocket. Additionally, it is widely recognized as one the most reliable software for protein-ligand docking.

AutoDock is a widely used software tool that performs molecular docking simulations to predict the binding affinity and orientation of a small molecule (the ligand) with a protein (the receptor). It is commonly used in drug discovery and computational biology research to help identify potential drug candidates or to gain insights into the molecular interactions between a ligand and a receptor.

Protein preparation for docking

Five important enzymes contribute to ZIKV cell invasion and infection, namely RNA-dependent RNA polymerase (PDB ID: 5WZ3 and 5U04), ZIKV Apo NS3h (PDB ID: 5JRZ), Axl Receptor (PDB ID 2C5D) and the human Axl protein (PDB ID: 5U6B). The three-dimensional structure of the proteins was obtained from the Protein Data Bank (www.PDB.org). Based on the location of the active sites, the docking grid boxes were then generated using AutoDock Tools v1.5.7.

The grid box was set at the volume of 40x40x40 with a spacing of 0.375 Å (default volume). The Autogrid calculation procedure was the place where we expressed the default values for the grid volume, a three–dimensional grid showed the protein, and each atom was placed at each grid point.

Ligand and energy minimization

To determine the energy minimization of ligand molecules, energy minimization of LIG molecules' rules force field in docking server was used. Partial charges to ligand atoms, combined non-polar hydrogen, atoms, and definite rotatable were assigned simultaneously. The ligands were downloaded from PubChem database (Bolton *et al.*, 2011).

In silico docking of compounds

In our study, ligands were selected and obtained data from some previous studies that extracted 53 phytochemicals from *E. prostrate* (Table S1). The 2D-structures of these phytochemicals were then converted into 3D-structures in PDB format using open babel (O'Boyle *et al.*, 2011) for molecular docking.

The ligands of phytochemical compositions of *E. prostrate* with targets proteins of Zika virus and human receptors were combined to determine their potential inhibitory effect on the virus. Our docking simulation was conducted using PyMOL Molecular Graphics, AutoDock Tools v1.5.7, and AutoDock Vina (Schrodinger, 2010; Trott, Olson, 2010)

Evaluation of ligands drug-likeness and toxicity

ADME parameters including absorption, drug delivery, metabolism, and excretion of a plant compound were predicted using a SwissADME web tool. Additionally, ADME characterization and drug similarity prediction of some anti-proliferative agents were performed in the preclinical drug discovery stage. In order to improve BBB (Blood-Brain Barrier) permeability through passive diffusion, five key physiochemical parameters (molecular weight ≤500, substance quantity, at least 10 hydrogen bonds donors, at least five hydrogen bond acceptors, a CLog P value ≤5, and a Polar Surface Area (PSA) <140 $Å^2$) need to be optimized, as stated in Lipinski's Rule of Five (Pollastri, 2010) (Figure 2.2). Furthermore, The pharmacokinetic properties of a given compound, such as substrate P-glycoprotein and inhibition of cytochrome P450 (CYP) isoenzymes 1A2, 2C19, 2C9, 2D6, and 3A4, were predicted using the SwissADME web tool (Daina, Michielin, & Zoete, 2017).

RESULTS AND DISCUSSION

Being screened compounds from *E. prostrata*

Prior to conducting docking, a total of fifty-three derivatives of *E. prostrata* were prepared and optimized (as shown in Table 1). The table demonstrates the vast array of chemical compounds that have been identified and isolated from *E. prostrata*, which includes alkaloids, triterpenoid saponins, phytosterols, flavonoids, coumestans, polypeptides, and lipids. Some of the major and important compounds found in *E. prostrata* are wedelolactone, ecliptasaponin A, luteolin, coumestans, polypeptides and phytosterols.

Molecular docking

Molecular binding simulations were conducted to assess the drug-like potential of various small molecules. The primary focus of these simulations was to evaluate the ability of these ligands to bind effectively to the active site of target proteins. The simulations revealed that increased positions/rotations resulted in better binding and interactions within the receptor. Based on their closeness to the original ligand site, the most valuable positions/rotations were selected. The results of the simulations were further analyzed, and Table 1 presents the interaction of free energies binding between proteins and ligands.

In order to predict the binding affinity between macromolecules and ligands in the study, the structures of important Zika viral proteins and plant metabolites were optimized for molecular binding. The resulting analysis, presented in Table 1, provided valuable insights into the interaction between these macromolecules and ligands. The top results based on binding energy showed that five ligands exhibited the same minimum binding energies for each macromolecule (Table 2). These findings suggest that these five ligands may be promising candidates for further investigation as potential therapeutics for Zika virus. However, additional studies will be needed to validate these results and determine the efficacy and safety of these ligands in vivo. The results of the experiments consistently showed that α-amyrin, echinocystic acid, eclalbasaponin I, ecliptasaponin A and ursolic acid demonstrated the strongest binding interaction with the Zika viral proteins and human target proteins (Table 2).

Table 1. Free energy of binding interaction (kcal/mol) between *Eclipta prostrata* compounds and target proteins.

Ligand	Target				
	5WZ3	5U04	5JRZ	2C5D	5U6B
Germacrene D	-6.2	-6.5	-6.1	-5.9	-6.0
(E) β-Farnesene	-5.1	-5.2	-4.8	-4.7	-5.1
(E-E) α-Farnesene	-5.1	-5.6	-4.8	-5.8	-5.4
A-Amyrin	-9.9	-9.2	-9.4	-8.0	-9.7
α-Humulene	-6.3	-6.6	-5.7	-5.9	-6.0
α-Santalene	-5.6	-6.3	-5.2	-4.9	-5.8
α-Thujene	-4.9	-5.0	-4.5	-5.0	-5.2
Apigenin	-7.6	-7.2	-7.3	-7.1	-7.3
Benzaldehyde	-4.0	-4.7	-5.0	-5.1	-5.1
β-Caryophyllene	-6.2	-6.4	-6.0	-5.6	-6.2
Borneol	-4.9	-5.1	-6.6	-4.9	-6.1
Camphene	-4.9	-4.9	-5.5	-4.8	-5.9
Camphor	-4.8	-5.0	-6.6	-4.9	-6.3
Caryophyllene oxide	-6.5	-6.9	-6.2	-5.6	-6.0
Cyclosativene	-6.0	-6.2	-5.9	-6.1	-5.7
Daucosterol	-8.8	-8.3	-8.6	-7.1	-8.1
Demethylwedelolactone	-8.3	-7.6	-7.8	-7.7	-7.8
Dodecane	-4.1	-4.3	-3.6	-3.5	-3.9
Gamma-Himachalene	-6.1	-6.6	-6.1	-6.1	-6.4
Germacrene B	-5.9	-6.3	-6.2	-5.9	-6.3
Humulene oxide II	-6.2	-6.2	-6.1	-5.7	-6.3
Isophorone	-5.0	-5.4	-5.6	-4.9	-6.0
Limonene	-4.8	-5.8	-4.7	-5.6	-5.3
Luteolin	-7.6	-7.3	-7.9	-7.4	-7.9
Luteolin 7-glucoside	-8.4	-8.3	-8.8	-7.5	-8.1
Myrcene	-4.4	-5.0	-4.6	-4.6	-4.7
n-Decane	-3.7	-4.6	-3.7	-3.4	-3.5
n-Eicosane	-4.5	-4.4	-4.5	-3.8	-4.0
n-Heptadecane	-4.0	-4.5	-3.8	-3.5	-4.4
n-Octadecane	-3.7	-4.7	-3.7	-4.1	-3.5

Nonanal	-3.5	-4.2	-3.7	-3.9	-3.6
n-Tridecane	-3.5	-4.3	-3.7	-3.8	-3.6
n-Undecane	-3.4	-4.5	-3.5	-3.2	-3.5
O-Cymene	-4.6	-5.6	-4.8	-5.1	-5.4
Oleanolic acid	-9.3	-8.6	-8.7	-7.7	-8.6
p-Cymene	-5.0	-5.9	-4.8	-5.7	-5.3
Pentadecanal	-3.8	-4.4	-4.0	-3.5	-3.9
Sativene	-5.9	-6.4	-5.8	-5.5	-6.1
Selina-3,7(11)-diene	-6.1	-6.5	-6.2	-5.9	-6.5
Silphiperfol-5-ene	-5.9	-6.6	-6.1	-5.7	-5.8
Stigmasterol	-8.0	-8.1	-7.6	-6.7	-7.0
Stigmasterol-3-O-glucoside	-9.5	-8.3	-8.0	-7.4	-7.3
Tetradecane	-4.1	-4.5	-3.7	-4.7	-3.9
Tricyclene	-4.5	-5.0	-6.2	-5.5	-5.5
Ursolic acid	-9.9	-8.9	-9.0	-8.1	-9.9
Wedelolactone	-7.9	-7.6	-8.0	-7.9	-7.8
Pratensein-7-O-glucopyranoside	-8.1	-7.6	-8.3	-7.5	-8.0
Ecliptasaponin A	-9.9	-9.5	-9.4	-8.6	-9.5
Echinocystic acid	-9.3	-10.0	-9.0	-7.8	-9.3
Eclalbasaponin I	-9.8	-9.2	-9.6	-7.6	-9.2
Diosmetin	-7.5	-7.4	-7.5	-6.7	-7.1
Isodemethylwedelolactone	-8.0	-7.3	-7.8	-7.3	-7.5
Coumestan	-7.5	-8.0	-7.1	-7.3	-7.2

Table 2. Analysis of binding energies and interaction sites of the best-screened compounds on target proteins.

Proteins (PDB)	**Ligands**	**binding enegy (kcal/mol)**	**Interaction sites**
2C5D	α-Amyrin	-8.0	Phe30, Cys49, Leu51, Glu56, Pro57, Glu59, Val60, Gln76, Gln78, Val91, Cys110, Val112,
	Echinocystic acid	-7.8	Phe30, Cys49, Leu51, Glu56, Pro57, Pro58, Glu59, Val60, Gln76, Gln78, Val91, Val92, Cys110, Val112

	Eclalbasaponin I	-7.6	Phe30, Cys49, Leu51, Val53, Pro57, Pro58, Val60, His61, Trp62, Gln76, Trp89, Val91, Gln109, Cys110, Val112
	Ecliptasaponin A	-8.6	Phe30, Leu51, Glu56, Pro57, Pro58, Glu59, Val60, His61, Gln78, Val91, Val92, Ser93, Leu111
	Ursolic acid	-8.1	Phe30, Cys49, Leu51, Pro57, Pro58, Glu59, Val60, Gln76, Gln78, Val91, Cys110, Val112
5JRZ	α-Amyrin	-9.4	Pro292, Ser293, Pro432, Leu442, Met536, Pro542, Val543, Arg598
	Echinocystic acid	-9.0	Ala264, Asp291, Met536, Pro542, Ala605
	Eclalbasaponin I	-9.6	Ser268, Pro292, Arg388, Met536, Asp540, Pro542, Val543, Ala604, Ala605
	Ecliptasaponin A	-9.4	Ser293, Met536, Asp540, Arg598, Ser601
	Ursolic acid	-9.0	Pro292, Pro432, Leu442, Met536, Pro542, Val543, Arg598
5U04	α-Amyrin	-9.2	Val606, Tyr609, Asn612, Ile799
	Echinocystic acid	-10.0	Val606, Tyr609, Ser712
	Eclalbasaponin I	-9.2	Val606, Thr608, Asn612, Ser 663, Asp665, Asp666, Ser798
	Ecliptasaponin A	-8.5	Tyr609, Ser712, Ser798, Ile799
	Ursolic acid	-8.9	Val606, Tyr609, Asn612, Trp797, Ile799
5U6B	α-Amyrin	-9.7	Phe547
	Echinocystic acid	-9.3	Phe547, Val550, Lys567, Asn677
	Eclalbasaponin I	-9.2	Phe547, Asn677, Pro712
	Ecliptasaponin A	-9.5	Phe547, Val550, Lys567
	Ursolic acid	-9.9	Phe547, Asp627, Ser630, Asp690
5WZ3	α-Amyrin	-9.9	Cys711, Trp797
	Echinocystic acid	-9.3	Arg483, Gln605, Val606, Tyr609
	Eclalbasaponin I	-9.8	Arg483, Asn494, Asp665, Val606, Ser712, Trp797, Ser798
	Ecliptasaponin A	-9.9	Arg483, Tyr609, Val606, Asp665 Cys711, Ser712, Trp797, Ser798
	Ursolic acid	-9.9	Gln605, Cys711, Trp797

Analysis and evaluation of compounds against ZIKV

The target protein of the Zika virus and the compounds from the *E. prostrata* (ligand) were optimized and molecularly bound to predict their binding affinity between the important target proteins and the mentioned ligand were shown in Table 2. Metabolomics results were based on the five highest scoring substances, and the minimum binding energies for each protein. Specifically, eclalbasaponin I exhibited the highest binding affinity for Human Axl Receptor (PDB:2C5D): -8.6 kcal/mol and ZIKV Apo NS3 Helicase (PDB:5JRZ) -9.6 kcal/mol, echinocystic acid with ZIKV NS5 RNA-dependent RNA polymerase (PDB: 5U04) −10 kcal/mol, ursolic acid with the human Axl protein (PDB: 5U6B) -9.9 kcal/mol and finally α-amyrin, ecliptasaponin A and ursolic acid together showed the best binding affinity for NS5 RNA-dependent RNA polymerase (RdRP) (PDB: 5WZ3) -9.9 kcal/mol.

To demonstrate the important drug surface position of the ZIKA proteins in the study, the structure of the binding complex was analyzed. The pattern of ligand binding and interacting radicals with their respective sites were shown in Table 2.

Toxicological analysis of the most potent compounds for drug development

Different properties of ADME including pharmacokinetics, lipophilicity, water solubility, and physicochemical and pharmacochemical parameters were calculated to determine leading drug candidates (Table 3).

Different properties of ADME including pharmacokinetics, lipophilicity, water solubility, and physicochemical and pharmacochemical parameters were calculated to determine leading drug candidates (Table 4). The findings indicate that drug metabolism is significantly influenced by six possible isozymes of P450, namely CYP1A2, CYP2C19, CYP2C9, CYP2D6, CYP2E1, and CYP3A4. The result also showed that none of the 5 potential isoforms were able to bind to any of cytochromes P450. Regarding GI absorption, echinocystic acid was found to have high adsorption while the remaining four substances, α-amyrin, eclalbasaponin I, ecliptasaponin A, and ursolic acid showed lower adsorption.

Table 3. Drug profiling and ADME analysis of the top five metabolites.

Parameters	α -Amyrin	Echinocystic acid	Eclalbasaponin I	Ecliptasaponin A	Ursolic acid
Physicochemical Parameters					
Molecular weight	426.72 g/mol	472.70 g/mol	796.98 g/mol	634.84 g/mol	456.70 g/mol
Num. rotatable bonds	0	1	7	4	1

No. H-bond acceptor	1	4	14	9	3
No. H-bond donors	1	3	9	6	2
TPSA	20.23 Å²	77.76 Å²	236.06 Å²	156.91 Å²	57.53 Å²
Lipophilicity					
Log Po/w (iLOGP)	4.77	3.47	3.60	3.60	3.71
Log Po/w (WLOGP)	8.02	6.20	1.29	3.64	7.09
Log Po/w (SILICOS-IT)	6.52	4.96	0.82	2.37	5.46
Pharmacokinetics					
GI absorption	Low	High	Low	Low	Low
BBB permeant	No	No	No	No	No
P-GP substrate	No	Yes	Yes	Yes	No
CYP1A2 inhibitor	No	No	No	No	No
CYP2C19 inhibitor	No	No	No	No	No
CYP2C9 inhibitor	No	No	No	No	No
CYP2D6 inhibitor	No	No	No	No	No
CYP3A4 inhibitor	No	No	No	No	No
Water Solubility					
Log S (ESOL)	-8.16	-7.04	-6.51	-6.51	-7.23
Solubility	2.94e-06 mg/ml; 6.89e-09 mol/l	4.32e-05 mg/ml; 9.14e-08 mol/l	2.45e-04 mg/ml; 3.08e-07 mol/l	1.94e-04 mg/ml; 3.12e-07 mol/l	2.69e-05 mg/ml; 5.89e-08 mol/l
Class	Poorly soluble	Poorly soluble	Poorly soluble	Poorly soluble	Poorly soluble

Log S (SILICOS-IT)	-6.71	-5.30	-1.65	-2.91	-5.67
Solubility	8.23e-05 mg/ml; 1.93e-07 mol/l	2.37e-03 mg/ml; 5.02e-06 mol/l	1.80e+01 mg/ml; 2.25e-02 mol/l	7.67e-01 mg/ml; 1.24e-03 mol/l	9.72e-04 mg/ml; 2.13e-06 mol/l
Class	Poorly soluble	Moderately soluble	Soluble	Soluble	Moderately soluble
Medicinal Chemistry					
Lipinski	Yes; 1 violation: MLOGP>4.15	Yes; 1 violation: MLOGP>4.15	No; 3 violations: MW>500, Nor O>10, NH or OH>5	No; 2 violations: MW>500, NH or OH>5	Yes; 1 violation: MLOGP>4.15
Leadlikeness	No; 2 violations: MW>350, XLOGP3>3.5	No; 2 violations: MW>350, XLOGP3>3.5	No; 1 violation: MW>350	No; 2 violations: MW>350, XLOGP3>3.5	No; 2 violations: MW>350, XLOGP3>3.5
Bioavailability Score	0.55	0.56	0.17	0.11	0.85
PAINS	0 alert	0 alert	0 alert	0 alert	0 alert

DISCUSSION

In light of this alarming outbreak, scientific activities have been accelerated in the past few years to explore viral pathogenesis, epidemiology, the biology of replication, and therapeutic targets for Zika virus (ZIKV) were conducted. Relying on these studies has partly expanded our understanding of ZIKV with the hope of finding appropriate treatment and prevention before the virus recurs. Among mosquito-borne human infections, ZIKV infection has the potential to become a worldwide pandemic (Yadav, Rawal, & Baxi, 2016). ZIKV infection can be transmitted from person to person by mother to child or through sexual contact. To date, despite the great efforts of scientists, there is no approved specific therapy against ZIKV or specific antiviral treatment for clinical ZIKV infection. It can be a challenge to develop anti-ZIKV agents.

Plants contain numerous phytochemicals with antioxidant effects, such as flavonoids, terpenoids, saponins, steroids, alkaloids, and coumarins which have been shown to inhibit viral activity. Pharmaceutical products based on plant-based products have fewer side effects and are less toxic to human health. Therefore, attempts have been made to examine several

plant-derived metabolites that inhibit ZIKA based on their binding to several important proteins. In the present study, 53 phytochemicals from *E. prostrata* were tested against five important ZIKA virus proteins, opening new opportunities for drug discovery and accelerated progress in this field (Hirono 2002). The In-Silico Docking method, which involves using computer simulations to predict how potential drug candidates bind to target proteins, has emerged as a promising tool for discovering and developing new lead compounds against various infectious pathogens, including ZIKA virus (Hirono 2002; Ivanov et al., 2006). This approach can save time and costs during drug development (Joseph et al., 2016). Several plant-derived compounds, such as α-amyrin, echinocystic acid, eclalbasaponin I, ecliptasaponin A and ursolic acid are potential antiviral agents against many important viruses.

The results of Table 2 showed that ecliptasaponin A exhibits the highest standardized energy (-8.6 kcal/mol) when it is bound to ZIKA Capsid (2C5D). Figure 1 illustrates the interaction diagram of ecliptasaponin A. Previous reports have confirmed significant interactions between ecliptasaponin A and the moieties of Phe30, Leu51, Glu56, Pro57, Glu59, Val60, His61, Gln78, Val91, Val92, and Leu111. This strong affinity is attributed to the hydrophilic active site, which is surrounded by hydrophilic amino acids like Cys, His, and Gln. Moreover, hydrogen bonds form between the radical His61 and the molecule's side chain OH groups. The molecule also engages in Alkin interactions with Pro58 and Val60, as well as other interactions (Figure 1).

Ursolic acid has been identified as the compound with the strongest binding energy for the human Axl protein (PDB: 5U6B). Compared to the other four compounds, ursolic acid demonstrates a higher affinity to the target protein, with a greater number of bonds formed. Notably, ursolic acid forms two hydrogen bonds between the amino acids Asp627 and Ser630 with OH groups, as well as a π-Alkyl interaction between Phe547 and the R group in the compound molecule. Additionally, some other weak effects occur (Figure 2) during ursolic acid's binding to the protein.

Table 3 revealed that echinocystic acid had the highest binding affinity to the NS5 RNA-dependent RNA polymerase, with an energy of -10.0 Kcal/mol. The active central region of the NS5 RNA polymerase (5U04) is surrounded by several hydrophilic amino acids, including Ser, Asp, Cys, Tyr, and Thr. Echinocystic acid attaches to the Oxygen group in the molecule, forming a strong hydrogen bond with the amino acid Ser712. In addition, interactions occur between the π-Alkyl, Alkyl in the R group (NH_3^+) and the benzene ring (Figure 3). It is worth noting that these interactions are crucial due to the short chain or hydrophilic group present in the compound.

Furthermore, numerous weak Van der Waals interactions are present around the echinocystic acid molecule. As a result, echinocystic acid generates a lower number of bonds with the NS5 RNA-dependent RNA polymerase in comparison to eclalbasaponin I and ecliptasaponin A. The structural size of the echinocystic acid molecule enables it to fit perfectly within the active site protein. In contrast, the remaining compounds, despite having the shape for more hydrogen bonds, also contain negative-negative and donor-donor interactions that could push the molecular structure out of the central region protein activity entrance.

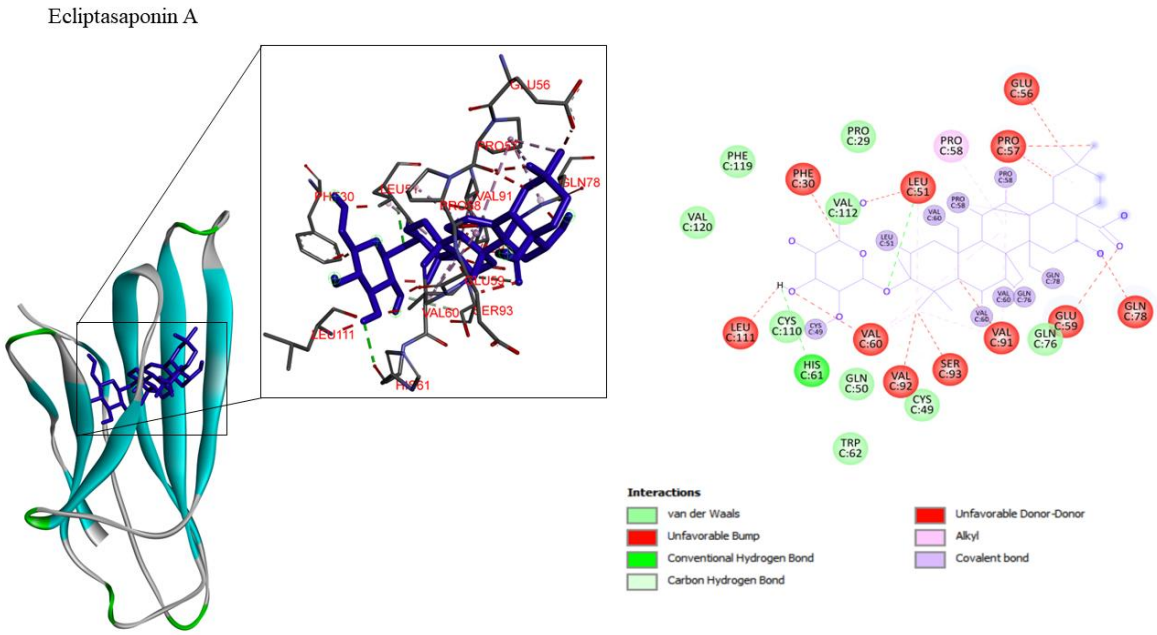

Figure 1. Ecliptasaponin A binding site on the active site of ZIKA Capsid (2C5D).

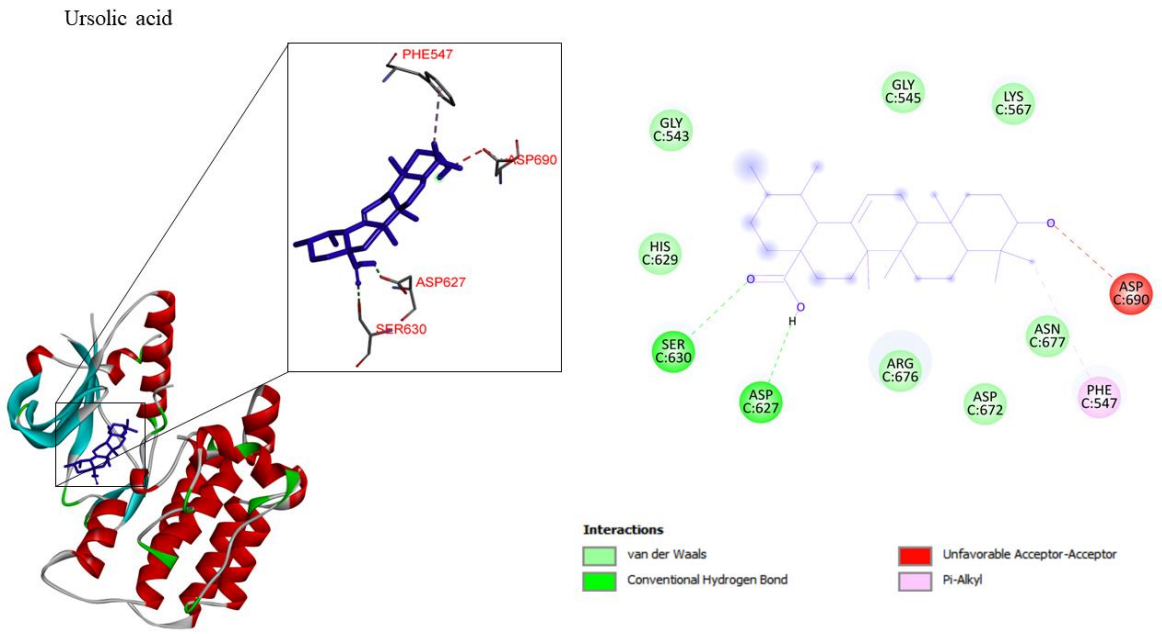

Figure 2. The ursolic acid binding site on the active site of the human Axl protein (PDB: 5U6B).

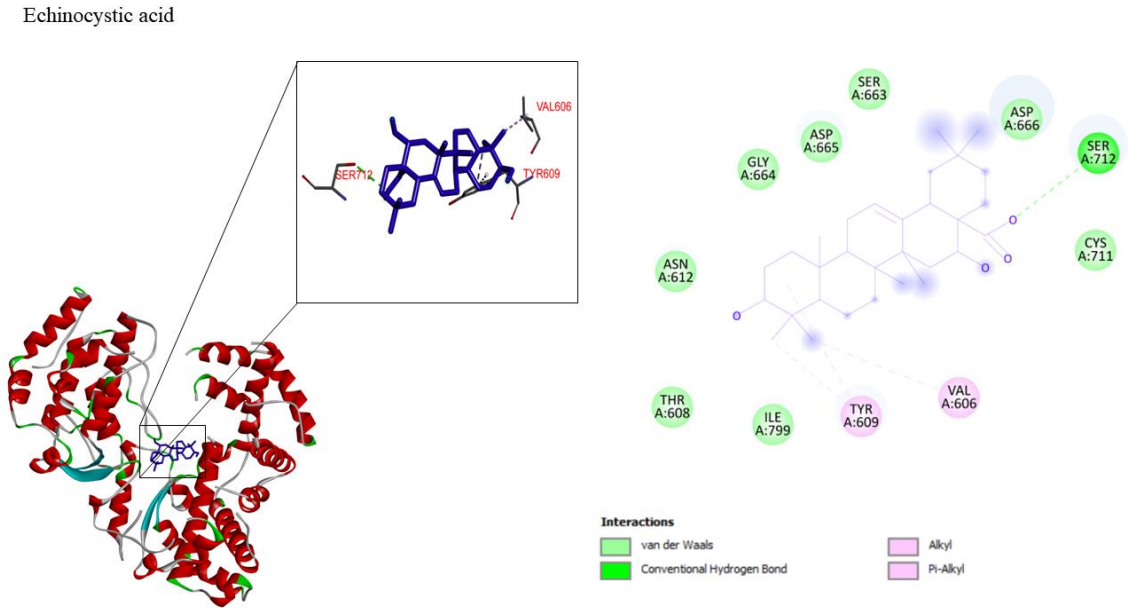

Figure 3. The Echinocystic acid binding site on the active site of NS5 RNA-dependent RNA polymerase (5U04).

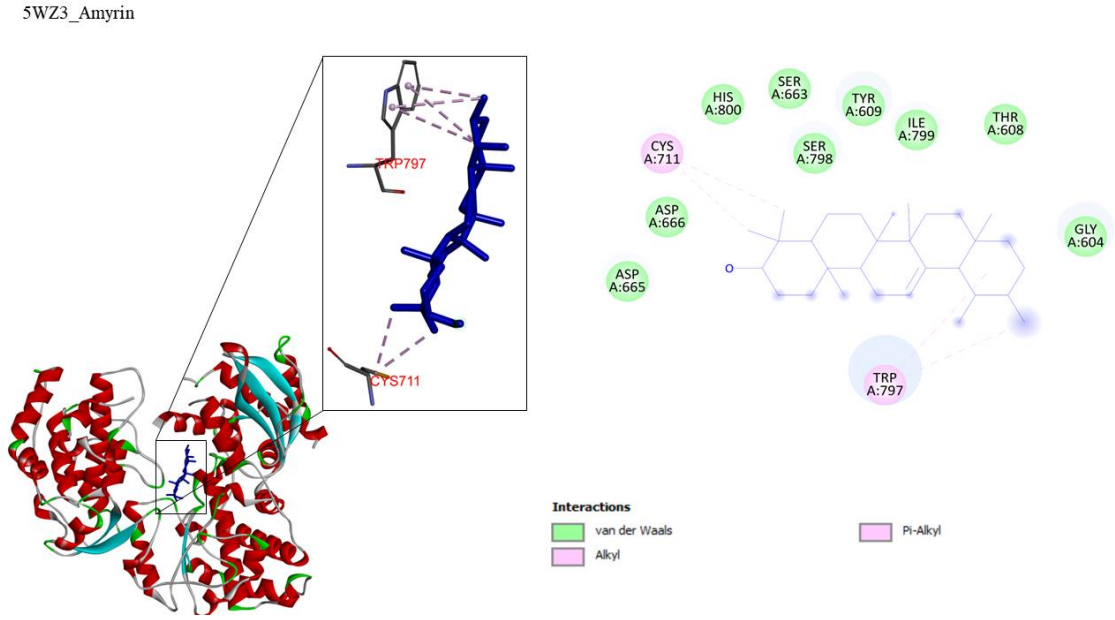

Figure 4. The α- Amyrin binding site on the active site of NS5 RNA-dependent RNA polymerase (5WZ3).

In this study, two different structures of NS5 RNA-dependent RNA polymerase proteins with PDB IDs (5U04) and (5WZ3) were utilized for molecular docking. Notably, there was a difference in the results between structures (5U04) and (5WZ3). The results

showed that α-amyrin, ecliptasaponin A, and ursolic acid had the highest binding energy (-9.9 kcal/mol) with the NS5 RNA-dependent RNA polymerase (5WZ3). It is worth noting that the active center of this enzyme is a hydrophilic region containing His, Cys, Asp, Ser, and Tyr, whereas α-Amyrin mainly forms π-amyrin interactions. Ecliptasaponin A, on the other hand, contains OH groups that form hydrogen bonds at Ser712, Arg483, Val606, and a π-Alkyl interaction at Tyr609, while ursolic acid forms hydrogen, π-Alkyl, and Alkyl bonds at OH, R (NH_3^+) groups, and benzene rings with Gnl605, Cys711, and Trp797, respectively. It is important to note that the binding energies of these compounds differ between the two NS5 RNA-dependent RNA polymerase structures.

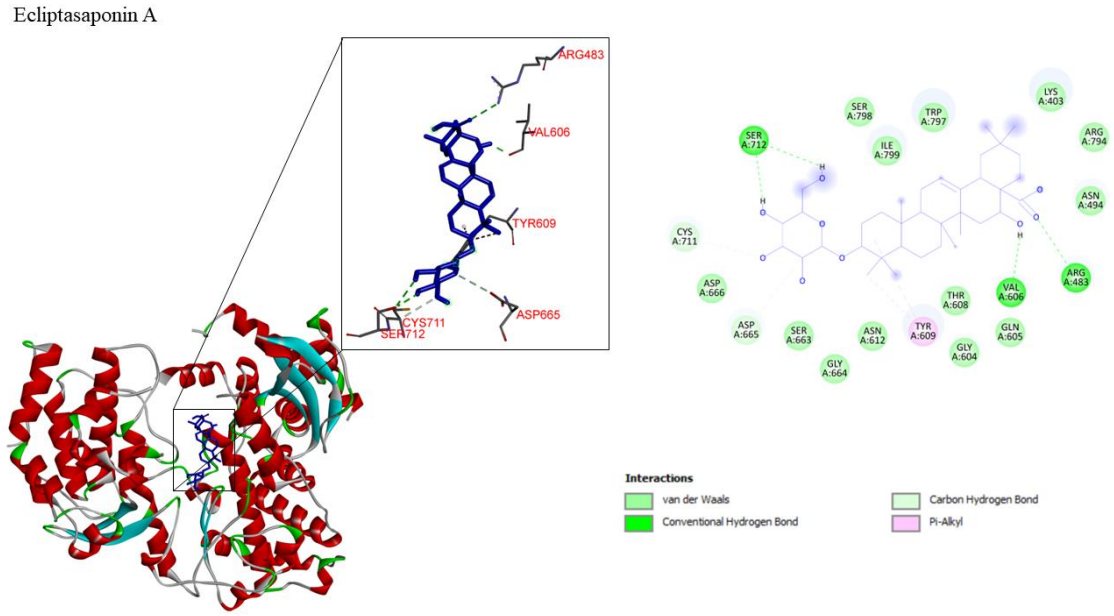

Figure 5. The Ecliptasaponin A binding site on the active site of NS5 RNA-dependent RNA polymerase (5WZ3).

Eclalbasaponin I showed strong binding to NS3h Apo ZIKV protein (5JRZ) through two water quality side chains. Specifically, the amino acids in the strategic binding and motion generation region linked with eclalbasaponin I, with Ser268 forming a hydrogen bond with the group and OH, and another hydrogen bond with one Oxygen group. Asp540 formed a hydrogen bond with the OH group on the circuit side of the water quality analog. These links were highly rigid. Additionally, many alkyl bonds were formed between the R groups (NH_3^+) and were present at positions Pro292, Val543, Pro542, Arg388, Ala604, and Ala605, along with many correlation factors around the protein entry and eclalbasaponin I (Figure 7).

Through ADME results, computer algorithms provide information about the processing or recognition of a substance when entering the body. Since then, the prediction of ADME and potential toxicity has been increasingly applied to reduce the number of animal tests.

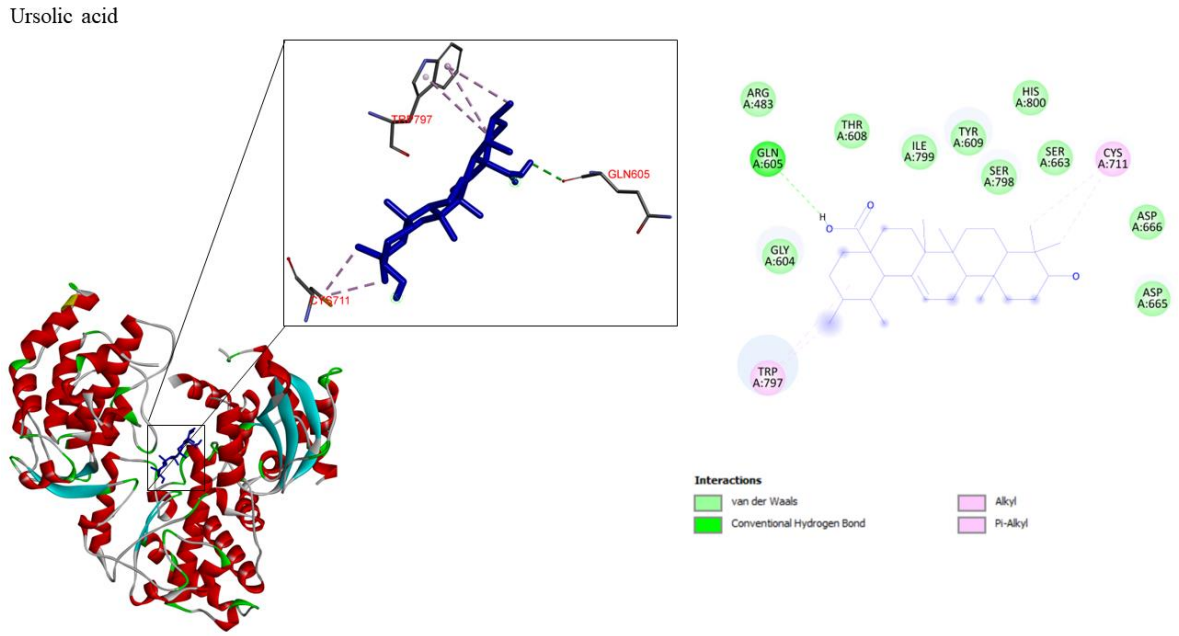

Figure 6. The Ursolic acid binding site on the active site of NS5 RNA-dependent RNA polymerase (5WZ3).

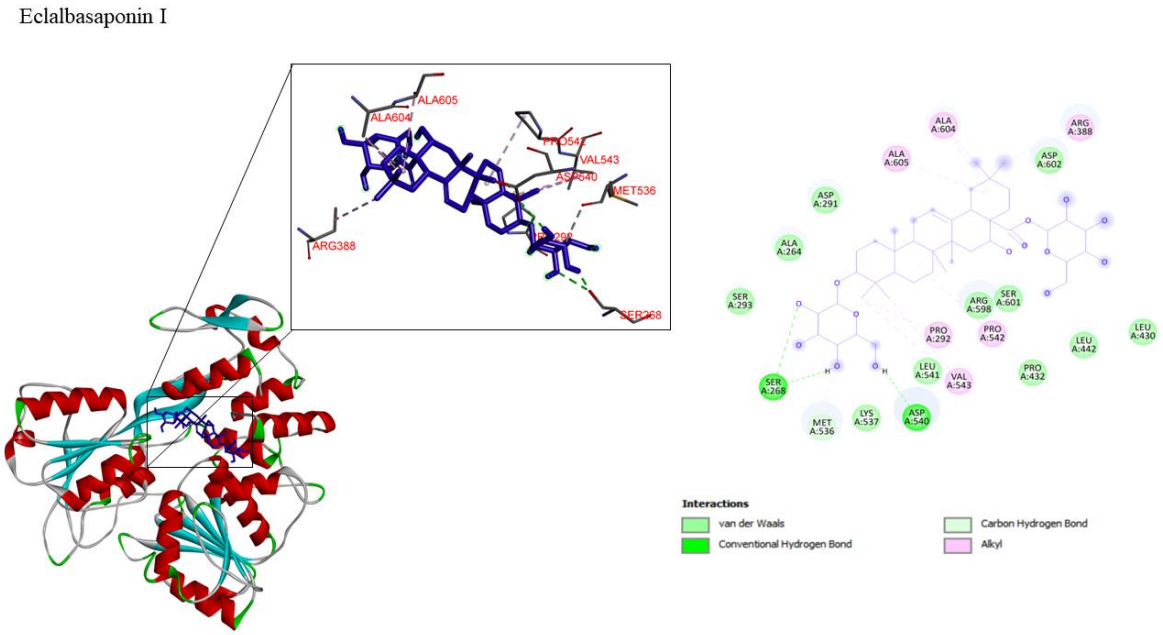

Figure 7. The Eclalbasaponin I binding site on the active site of NS3h Apo ZIKV (5JRZ).

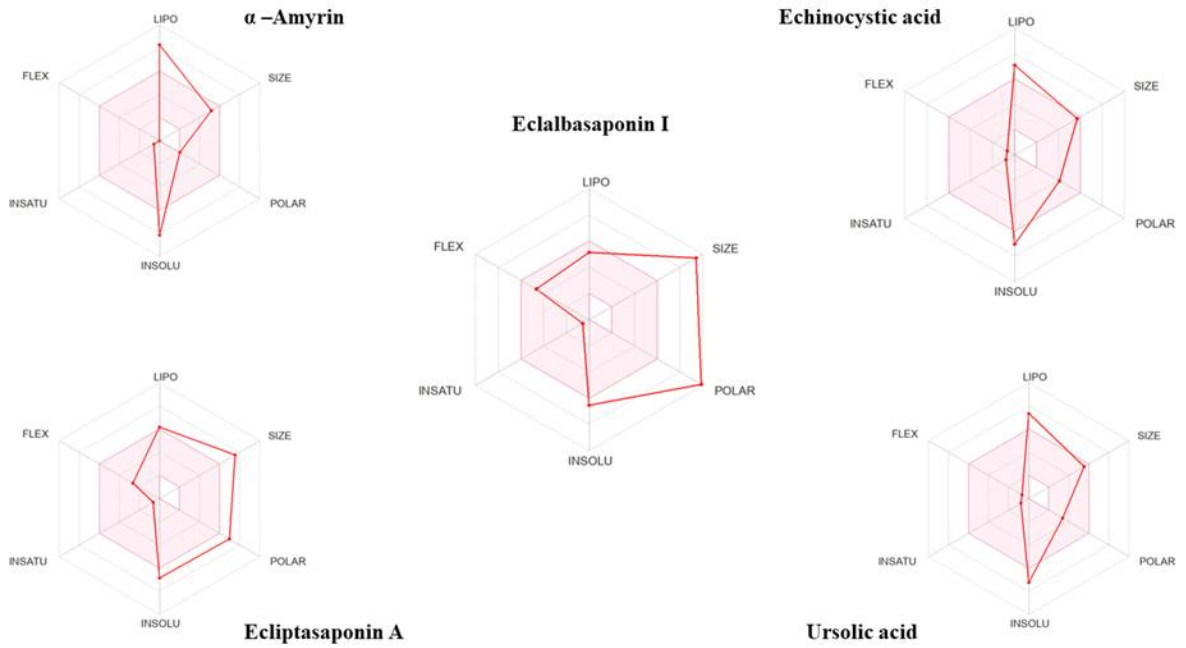

Figure 8. The bioavalability radar for a-amyrin, ecliptasaponin A, eclalbasaponin I, echinocystic acid and ursolic acid

Among the six isozymes, CYP3A4 has led to various drug-drug interactions with significant clinical implications. While the majority of isozymes are located in the liver, extrahepatic metabolism also takes place in other organs such as the kidneys, skin, gastrointestinal tract, and lungs. The CYP3A4 isozyme extensively metabolizes certain oral drugs during the first pass in the gastrointestinal tract, leading to their inactivation. In Table 3, all five of the top compounds analyzed in the study showed no drug interactions. Therefore, it is crucial to discover drugs that can predict a molecule's potential to induce significant drug interactions by inhibiting CYP and determine the affected isoforms.

SwissADME can be used to predict whether a chemical is a substrate of P-GP or an inhibitor of the most important CYP isoenzymes. The statistical performance of classification models suggests that three compounds displaying inhibitory ability: echinocystic acid, eclalbasaponin I, and ecliptasaponin A (Table 3). In contrast α-amyrin and ursolic acid did not show any results. It is apparent that eclalbasaponin I and ecliptasaponin A violated more than two criteria of the five rules of Lipinski, indicating that they have poor absorption and are impermeable. This suggests that only the remaining three compounds are highly pharmacologically active. Figure 8 provides an overview of a molecule's drug-like properties. The pink area on the radar chart denotes the range for each property. The analysis showed that eclalbasaponin I and ecliptasaponin A were within the optimal range for each physicochemical property, lipophilicity (-0.7 < XLOGP3 < 5.0). On the other hand, α-amyrin, echinocystic acid, and ursolic acid have suboptimal properties in terms of size (150 g/mol < MV < 500 g/mol), polarity (20 $Å^2$ < TPSA < 130 $Å^2$), and

flexibility. However, all five substances have optimal flexibility (0 < Number of rotating bonds < 9). The analysis also showed that none of the five substances were highly soluble, with a suboptimal index (0 < Log S (ESOL) < 6), and they did not have an optimal saturation (0.25 < Csp3 fraction < 1). Therefore, the best derivatives present in *E. prostrata* are likely to be orally absorbed, but not to a high degree.

CONCLUSION

The main focus of this study is to investigate the compounds found in *E. prostrata* for their potential inhibition of various targets, including ZIKV NS5 RNA-dependent RNA polymerase (PDB ID: 5WZ3 and 5U04), ZIKV Apo NS3 helicase (PDB ID: 5JRZ), human Axl Receptor (PDB ID 2C5D), and human Axl protein (PDB ID: 5U6B). The results showed that ecliptasaponin A is a potential inhibitor of human Axl Receptor, eclalbasaponin I inhibits ZIKV Apo NS3 helicase, ursolic acid inhibits human Axl protein, and echinocystic acid inhibits RNA-dependent RNA polymerase (5U04). Furthermore, amyrin, ecliptasaponin A, and ursolic acid are potential inhibitors of RNA-dependent RNA polymerase (5WZ3).

The study's results are significant as they indicate that the natural derivatives identified in this study have the potential to act as inhibitors against the ZIKV. This finding is promising and provides a basis for further experimental studies to explore the potential of these compounds in treating ZIKV infections. The discovery of these potential inhibitors also creates an opportunity to design and develop new candidates with better inhibitory activity against ZIKV. This could lead to the development of more effective treatments for ZIKV infections and contribute to the advancement of the pharmaceutical industry.

Overall, this study represents a significant step forward in the search for new and effective treatments against the Zika virus. The findings provide a strong foundation for further research in this area and offer hope for those affected by this devastating virus.

Acknowledgement: *The author sincerely appreciates the support of the Department of Science and Technology of Tra Vinh Province (Grant Number: 07/HĐ-SKHCN).*

REFERENCES

Bolton EE, Chen J, Kim S, Han L, He S, Shi W, Simonyan V, Sun Y, Thiessen PA, Wang J, Yu B, Zhang J, Bryant SH (2011) PubChem3D: a new resource for scientists. *J Cheminform* 3: 1-15.

Daina A, Michielin O, Zoete V (2017). SwissADME: a free web tool to evaluate pharmacokinetics, drug-likeness and medicinal chemistry friendliness of small molecules. *Sci Rep* 7(1), 42717.

Dick GW, Kitchen S, Haddow A (1952) Zika virus (II). Pathogenicity and physical properties. *Trans R Soc Trop Med Hyg* 46(5).

Haddow AJ, Williams MC, Woodall JP, Simpson DI, Goma LK (1964) Twelve isolations of Zika virus from Aedes (Stegomyia) africanus (Theobald) taken in and above a Uganda forest. *Bull World Health Organ* 31(1), 57.

Liu QM., Zhao HY, Zhong XK & Jiang JG (2012). Eclipta prostrata L. phytochemicals: isolation, structure elucidation, and their antitumor activity. *Food Chem Toxicol* 50(11), 4016-4022.

Macnamara F (1954) Zika virus: a report on three cases of human infection during an epidemic of

jaundice in Nigeria. *Trans R Soc Trop Med Hyg* 48(2): 139-145.

Marchette N, Garcia R, Rudnick A (1969) Isolation of Zika virus from Aedes aegypti mosquitoes in Malaysia. *Am J Trop Med Hyg* 18(3).

Maslow JN, Roberts CC (2020) Zika virus: a brief history and review of its pathogenesis rediscovered. *Zika Virus: Methods Protoc*: 1-8.

O'Boyle NM, Banck M, James CA, Morley C, Vandermeersch T, Hutchison GR. (2011). Open Babel: An open chemical toolbox. *J Cheminform* 3(1), 1-14.

Ogunbinu AO, Flamini G, Cioni PL, Ogunwande IA, Okeniyi SO (2009) Essential oil constituents of Eclipta prostrata (L.) L. and Vernonia amygdalina Delile. *Nat Prod Commun* 4(3), 1934578X0900400321.

Pollastri MP (2010) Overview on the Rule of Five. *Curr Protoc Pharmacol* 49(1), 9.12. 11-19.12. 18.

Schrodinger L (2010) The PyMOL molecular graphics system, version 1.3 r1.

Trott O, Olson AJ (2010) AutoDock Vina: improving the speed and accuracy of docking with a new scoring function, efficient optimization, and multithreading. *J Comput Chem* 31(2): 455-461.

Yadav S, Rawal G & Baxi M. (2016). Zika virus: a pandemic in progress. *J Transl Intern Med* 4(1): 42-45.

Supplementary Data:

Table S1. Main phytocompounds in *Eclipta prostrata*

Name	Abbreviation	Formula	Group
Germacrene D	GMD	$C_{15}H_{24}$	Hydrocarbon
(E)-b-Farnesene	EBF	$C_{15}H_{24}$	Hydrocarbon
(E, E)-α-Farnesene	aFar	$C_{15}H_{24}$	Hydrocarbon
α-Amyrin	αAm	$C_{30}H_{50}O$	Triterpene
α-Humulene	HUM	$C_{15}H_{24}$	Sesquiterpene
α-Santalene	αSTL	$C_{15}H_{24}$	Sesquiterpene
α-Thujene	αTE	$C_{10}H_{16}$	Monoterpene
Apigenin	Age	$C_{15}H_{10}O_5$	Flavonoid
Benzaldehyde	BAL	C_7H_6O	Aldehyde
b-Caryophyllene	BCP	$C_{15}H_{24}$	Sesquiterpene
Borneol	BOR	$C_{10}H_{18}O$	Terpenoid
Camphene	CMP	$C_{10}H_{16}$	Monoterpens
Camphor	CA	$C_{10}H_{16}O$	Terpenoid
Caryophyllene oxide	CPO	$C_{15}H_{24}O$	Epoxide
Cyclosativene	CSV	$C_{15}H_{24}$	Sesquiterpenoids
Daucosterol	DS	$C_{35}H_{60}O_6$	Steroidsaponin
Demethylwedelolactone	DWEL	$C_{15}H_8O_7$	Coumestan
Dodecane	DD	$C_{12}H_{26}$	Hydrocarbon
g-Himachalene	γHCL	$C_{15}H_{24}$	Sesquiterpenoids
Germacrene B	GMB	$C_{15}H_{24}$	Sesquiterpenes
Humulene oxide II	HLO	$C_{15}H_{24}O$	Hydrocarbon
Isophorone	IPR	$C_9H_{14}O$	Cyclic ketone

Limonene	LM	$C_{10}H_{16}$	Cyclic monoterpene
Luteolin	LU	$C_{15}H_{10}O_6$	Flavonoid
Luteolin 7-glucoside	L7G	$C_{21}H_{20}O_{11}$	Flavonoid
Myrcene	MC	$C_{10}H_{16}$	Monoterpene
n-Decane	nDEC	$C_{10}H_{22}$	Hydrocarbon
n-Eicosane	nECS	$C_{20}H_{42}$	Hydrocarbon
n-Heptadecane	nHTD	$C_{17}H_{36}$	Hydrocarbon
n-Octadecane	nOTD	$C_{18}H_{38}$	Hydrocarbon
Nonanal	NN	$C_9H_{18}O$	Aldehyd
n-Tridecane	nTDC	$C_{13}H_{28}$	Hydrocarbon
n-Undecane	nUDC	$C_{11}H_{24}$	Hydrocarbon
O-Cymene	o-CYM	$C_{10}H_{14}$	Hydrocarbon
Oleanolic acid	OA	$C_{30}H_{48}O_3$	Triterpenoid pentacyclic
p-Cymene	p-CYM	$C_{10}H_{14}$	Monoterpene
Pentadecanal	PDC	$C_{15}H_{30}O$	Aldehyde
Sativene	STV	$C_{15}H_{24}$	Sesquiterpene
Selina-3,7(11)-diene	S3,7D	$C_{15}H_{24}$	Sesquiterpene
Silphiperfol-5-ene	S5E	$C_{15}H_{24}$	Hydrocarbon
Stigmasterol	STG	$C_{29}H_{48}O$	Phytosterol
Stigmasterol -3-O-glucoside	S3G	$C_{35}H_{58}O_6$	Phytosterol
Tetradecane	TDC	$C_{14}H_{30}$	Hydrocarbon
Tricyclene	TC	$C_{10}H_{16}$	Monoterpene
Ursolic acid	UA	$C_{30}H_{48}O_3$	Pentacyclic triterpenoid
Wedelolactone	WEL	$C_{16}H_{10}O_7$	Coumestan
Pratensein-7-O-	P7G	$C_{22}H_{22}O_{11}$	Phytosterol

glucopyranoside			
Ecliptasaponin A	ESA	$C_{36}H_{58}O_9$	Triterpenoid saponin
Echinocystic acid	ECA	$C_{30}H_{48}O_4$	Triterpenoid.
Diosmetin	DMT	$C_{16}H_{12}O_6$	Monomethoxy
Eclalbasaponin I	EBS I	$C_{42}H_{68}O_{14}$	Flavone
Isodemethylwedelolactone	IDWEL	$C_{15}H_8O_7$	Triterpenoid saponin
Coumestan	CMT	$C_{15}H_8O_3$	Coumestan